



Leveraging the Thermoresponsiveness of Poly(N-Isopropylacrylamide) Copolymers as a Sensing Tool for Perfluorooctane Sulfonate

Journal:	<i>Analyst</i>
Manuscript ID	AN-ART-01-2021-000144.R1
Article Type:	Paper
Date Submitted by the Author:	06-Apr-2021
Complete List of Authors:	Savage, Dustin; University of Kentucky College of Engineering, Department of Chemical and Materials Engineering Hilt, J.; University of Kentucky College of Engineering, Chemical and Materials Engineering Dziubla, Thomas; University of Kentucky College of Engineering, Chemical and Materials Engineering

ARTICLE

Leveraging the Thermoresponsiveness of Poly(*N*-Isopropylacrylamide) Copolymers as a Sensing Tool for Perfluorooctane Sulfonate

Received 00th January 20xx,
Accepted 00th January 20xx

DOI: 10.1039/x0xx00000x

Dustin T. Savage,^a J. Zach Hilt^a and Thomas D. Dziubla^{*a,b}

Due to mounting evidence of the negative health effects of persistent perfluoroalkyl acids (PFAAs) with long (i.e., >C₇) tails, there is a need for convenient systems capable of sensing these contaminants at dilute aqueous concentrations. To address this concern, a thermoresponsive polymeric network composed of poly(*N*-isopropylacrylamide) copolymerized with fluorinated comonomers was studied to characterize the gel's physical response to fluorosurfactants in solution. Incorporating fluorinated comonomers into the polymer backbone raised their swelling in fluorocontaminant solutions relative to water – gels synthesized with 10.0 mol% 2,2,2-trifluoroethyl acrylate (TFEA) displayed a heightened maximum water-analyte swelling difference of 3,761 ± 147% compared to 3,201 ± 466% for non-fluorinated gels in the presence of 1 mM tetraethylammonium perfluorooctane sulfonate (TPFOS). The normalized area under the curve for gels with 12.5 mol% TFEA was further raised to 1.77 ± 0.09, indicating a broadened response window for the contaminant, but at the cost of reducing the overall swelling ratio to 3,227 ± 166% and elongating the time required to reach swelling equilibrium. Overall, a copolymer fed with 10.7 mol% TFEA was predicted to maximize both the swelling and response window of the polymer toward TPFOS. Equilibration times followed a logarithmic increase as the percentage of comonomer was raised, noting gradual fluorosurfactant penetration into the gels impeded by initial gel compaction caused by the addition of fluorinated comonomers. Comparative study of gels containing 1*H*,1*H*,7*H*-dodecafluoroheptyl acrylate, TFEA, or 1,1,1,3,3,3-hexafluoroisopropyl acrylate identified careful selection of fluorinated comonomers and their feed ratios as useful tools for tailoring the network's swelling response to TPFOS.

1. Introduction

Fluorosurfactants present a distinct challenge for environmental remediation efforts. Their unique properties that make them useful as interfacial stabilizers¹ also prevent their degradation and generate concern for their potential health impacts.² The strength of their carbon-fluorine bonds makes their fluorinated tails chemically and thermally resistant, leading to prolonged lifetimes in the environment, promoting bioaccumulation.³ Adding to their ubiquity,^{4, 5} annual emission estimates for C₄-C₁₄ perfluorocarboxylic acids (PFCAs), a subset of per- and polyfluoroalkyl substances (PFAS), ranged between about 55 tonnes/yr and 520 tonnes/yr from 2003 to 2015 with substantial variability across time.⁶ From the onset of PFAS production in 1951 to 2015, the total level of PFCA emissions spans 2,610 tonnes to 21,400 tonnes with another 20 tonnes to 6,420 tonnes projected for 2016 to 2030.⁶ Combined with another 4,481 tonnes of perfluorooctane sulfonate (PFOS) produced by 2000 and 96,000

tonnes of perfluorooctane sulfonyl fluoride in use by 2017,⁷ the staggering number of perfluoroalkyl acids (PFAAs) in circulation has helped inflate the growing list of at least 4,730 chemicals documented under the PFAS umbrella.⁸ Taking these estimates as measures of direct or indirect release or stockpiles with the potential for eventual release, the surfeit of PFAS comprises a major problem for extraction and analytical sectors to manage. To address this issue, our previous work⁹ explored the association of two particularly alarming PFAAs, perfluorooctanoic acid (PFOA) and PFOS, to a highly studied thermoresponsive polymer, poly(*N*-isopropylacrylamide) (PNIPAM), as a possible means for creating a facile polymeric sensing system for the contaminants. From that study, PFOS was shown to significantly alter the swelling and lower critical solution temperature (LCST) of PNIPAM hydrogels at a concentration equal to or more dilute than PFOA and other common swelling disrupters, leading to considerations for potential improvement of the polymer to enhance its swelling response to the analyte of interest.

As a way to tune the network's swelling to PFOS, the addition of fluorinated comonomers into the network was hypothesized to result in fluorine-fluorine attraction and reduce interaction with non-fluorinated analytes. Together, these contributions along with the weak polyelectrolytic character of PNIPAM would augment the gels' swelling response by lowering the concentration at which fluorosurfactants associate with the network and, consequently,

^a University of Kentucky, College of Engineering, 512 Administration Drive, 177 F. Paul Anderson Tower, Lexington, KY 40506

^b Email: thomas.dziubla@uky.edu

Electronic Supplementary Information (ESI) available: [details of any supplementary information available should be included here]. See DOI: 10.1039/x0xx00000x

destabilize the hydration shell surrounding PNIPAM or accelerate multilayering with electrostatic repulsion. Perturbations resulting from these phenomena relative to non-fluorinated analogs potentially offer a route for lowering the detection limits of systems employing these gels. To test this hypothesis, three fluorinated comonomers representing different structural arrangements, a pendent trifluoro group (2,2,2-trifluoroethyl acrylate, TFEA), a C₇ fluorinated chain (1*H*,1*H*,7*H*-dodecafluoroheptyl acrylate, DFHA), and branching (1,1,1,3,3,3-hexafluoroisopropyl acrylate, HFIA), were selected for copolymerization. Assessing the incorporation of the fluorinated groups into the polymer backbone along with the swelling behavior of each copolymer provides the basis for identifying an optimal copolymer designed for fluorinated analytes that will constitute the groundwork for improving forthcoming polymeric strategies for addressing contamination from perfluorinated chemicals.

2. Methods

2.1 Materials

Unless noted otherwise, all reagents were used as received without further purification. Monomers used throughout the syntheses were *N*-isopropylacrylamide (NIPAM, Sigma, 97%), 2,2,2-trifluoroethyl acrylate (TFEA, TCI, 98%, stabilized with 4-methoxyphenol), 1*H*,1*H*,7*H*-dodecafluoroheptyl acrylate (DFHA, Alfa, 97%, stabilized with 50 ppm 4-methoxyphenol), and 1,1,1,3,3,3-hexafluoroisopropyl acrylate (HFIA, Matrix, 99%). Gels were crosslinked with *N,N'*-methylenebis(acrylamide) (MBA, Sigma, 99%) and synthesized using the free radical photoinitiator 2-hydroxy-4'-(2-hydroxyethoxy)-2-methylpropiophenone (I2959, TCI, 98%). Phenol (Ph, Fluka, 99%), octanoic acid (OA, Alfa, 98%), methanol (MeOH, Pharmco, HPLC-UV grade), sodium dodecyl sulfate (SDS, VWR Chemicals, biotechnology grade), sodium octyl sulfonate (SOS, TCI, 98%), perfluorooctanoic acid (PFOA, TCI, 98%), tetraethylammonium perfluorooctane sulfonate (TPFOS, BeanTown Chemical, 98%), and potassium perfluorobutane-1-sulfonate (PFBS, Sigma, synthesis grade) were used as analytes for swelling tests. Dimethyl sulfoxide (DMSO, Pharmco, reagent ACS grade), acetone (Pharmco, reagent ACS/USP/NF grade), and deionized (DI) water (1 M Ω) were used as solvents in their respective experiments. Both DMSO and MeOH were stored over 3 Å molecular sieves to minimize residual water. Structures of the various chemicals used are provided in Supplementary Figure 1.

2.2 Hydrogel Synthesis

All syntheses were conducted in the manner described previously.⁹ Briefly, for a gel synthesized with 5 mol% DFHA, 0.752 mL (0.096 mmol) from a 19.681 mg/mL stock solution of MBA was added to a 20 mL scintillation vial containing 0.430 g (3.803 mmol) of NIPAM and 1.577 mL of anhydrous DMSO as a suitable solvent for all polymerization components. Another 75.32 μ L (0.195 mmol) of DFHA was injected followed by 0.175 mL (0.037 mmol) from a 47.951 mg/mL stock solution of I2959. The solution was mixed, inserted between glass sheets separated by a 0.51 mm thick polypropylene spacer, and cured with UV light at 5.00 mW/cm² for 1 h. The set gel was transferred to a jar holding 200 mL DI water and soaked for 2 h under 50 rpm shaking. The water was replaced

with fresh water and the cycle repeated for a total of five washes. Washed hydrogels were portioned into disks with a 6.95 mm punch and lyophilized. Gels synthesized with ≥ 10 mol% TFEA were soaked in acetone for approximately 1 min before cutting and disks were air dried overnight prior to lyophilizing. Dry gel disks were then used for subsequent swelling analyses. Conditions used for each gel variant are provided in Table 1.

2.3 Characterization

Fourier-transform infrared spectroscopy (FTIR) and X-ray photoelectron spectroscopy (XPS) were utilized to check comonomer incorporation in the synthesized gels. Attenuated total reflectance (ATR)-FTIR spectra were collected with a Varian 7000e FT-IR Spectrometer set to a resolution of 8 cm⁻¹ co-added over 32 scans at a speed of 5 kHz. Elemental analysis was performed on each gel with a K-Alpha XPS (Thermo Scientific) using a spot size of 400 μ m for a binding energy survey from -10 to 1,350 eV with a pass energy of 200 eV. The energy step size was held at 1 eV across 10 scans with a 10 ms dwell time. Two spots on opposite ends of each sample were captured to monitor intrabatch heterogeneity, and data represents the average and standard deviation from the two points for each gel between three gels synthesized identically. Linescans were drawn along the central z-axis of split T35.0 samples with a spot size of 30 μ m. Six spots were planted equidistant from one another along the length of the scan, permitting three reflected points for each disk spanning from the thickness's center. Parameters for surveys collected across the line scan were the same as those used for surface surveys.

2.4 Swelling Studies

Swelling assessments were conducted similarly to the method used previously.⁹ Solutions of 1 mM SDS, SOS, OA, and Ph, 10 mM MeOH, and 1 mM PFOA with 10 mM MeOH were kept at 5 °C in an LKB Bromma 2219 Multitemp II Thermostatic Circulator for 72 h prior to taking their first mass measurement, and subsequent measurements were recorded 24 h after incrementing the bath temperature by 2.5 °C. Gels incubated with TPFOS other than those fed with 20 mol% TFEA (T20.0) were initially equilibrated for 1,128 h before their first measurement. T20.0 samples were held for 1,656 h (see Supplementary Figure 2). TPFOS samples followed the same 24 h equilibration between temperature ramps as for the other analytes. Titration samples were initially held at 20 °C for 16 h before data collection, and 24 h was allotted before recording after ramping the temperature to 35 °C and 45 °C. Kinetic analyses were maintained at 5 °C throughout their duration.

Swelling ratios (Q) were calculated from the initial dry disk mass (m_i) and the swollen mass (m_s) at a specific temperature following $Q = m_s/m_i$. The water-analyte swelling difference (σ) for a given gel was determined from the swelling ratio of the hydrogel exposed to a given concentration of analyte at a specified temperature (Q_A) compared to its swelling ratio in water at the same temperature (Q_W) with $\sigma = (Q_A - Q_W)/Q_W \cdot 100\%$. Normalized area under the curve (AUC) was computed using the trapezoidal rule for each point along the σ curve between 5 °C and 50 °C referenced against the BG AUC. LCST estimates were drawn from linear interpolation of the temperature at which half the sum of the maximum and minimum swelling ratio lies.

3. Results

3.1 Synthesis & Characterization

Fluorinated comonomers were successfully incorporated into the backbone of PNIPAM hydrogels by formulating the syntheses in an organic solvent (DMSO) suitable for all monomers (NIPAM, MBA, DFHA, TFEA, and HFIA) and the initiator (I2959) used. Gels with high fluorine content (≥ 10 mol% TFEA) subject to reswelling in acetone prior to cutting and drying in ambient conditions formed small (roughly 3.25 mm diameter, 0.26 mm thickness), translucent disks, whereas lower fluorine feedstocks that were punched after swelling in water formed larger (about 5.64 mm diameter, 0.52 mm thickness for BG samples), opaque disks with varying diameters and thicknesses, which varied based upon the comonomer used (see Supplementary Figure 3). For polymers generated with the pendent trifluoro group comonomer, characteristic vibrational bands at $1,639\text{ cm}^{-1}$ and $1,539\text{ cm}^{-1}$ (see Supplementary Figure 4) mark the amide I (A1) and amide II peaks for PNIPAM,¹⁰ and the downfield peak at $1,755\text{ cm}^{-1}$ represents the carbonyl signature from TFEA.¹¹⁻¹³ Shallow peaks at $1,281\text{ cm}^{-1}$ and 976 cm^{-1} correspond to C-F stretching¹³ and CF_3 absorption or C-H bending, respectively.^{13, 14} The latter band could also be due to $\text{CH}=\text{CH}_2$ wagging,¹¹ an artifact from water washing highly fluorinated copolymers, but the transmittance relative to the baseline adjacent to the peak at $1,003\text{ cm}^{-1}$ forms a linear relationship ($r^2 = 0.987$) throughout the TFEA molar feed ratios applied. Were the peak due to residual comonomer, significant accrual would be expected at the higher extreme of TFEA feeds in a, perhaps, logarithmic rather than linear fashion. The CF_x absorption from $1,173\text{ cm}^{-1}$ to $1,153\text{ cm}^{-1}$ is readily apparent in each TFEA polymer,^{12, 14} and the ratio of this peak to the A1 band from NIPAM (see Supplementary Figure 5) forms a fairly linear relation ($r^2 = 0.943$) across the range of TFEA feed ratios employed.

Gels synthesized with DFHA have markedly similar peak distributions to those with TFEA, but with branching of the CF_x absorption band from $1,173\text{ cm}^{-1}$ to $1,153\text{ cm}^{-1}$ into three nearby peaks at $1,200\text{ cm}^{-1}$, $1,169\text{ cm}^{-1}$, and $1,134\text{ cm}^{-1}$ assigned to CF_2H , CF_2 , and CH_2CF_2 absorptions, respectively. Those with HFIA show even more convoluted fingerprint regions with absorptions at $1,234\text{ cm}^{-1}$, $1,200\text{ cm}^{-1}$, $1,173\text{ cm}^{-1}$, $1,130\text{ cm}^{-1}$, and $1,111\text{ cm}^{-1}$ due to symmetric (upfield) and asymmetric (downfield) stretching of the branched CF_3 groups. The individuality of each spectrum combined with consistent amide signatures indicates successful copolymerization of NIPAM and each fluorinated comonomer.

Surface elemental analysis from XPS shown in Figure 1 (a) confirmed fluorine addition to the networks but with substantial variations from their anticipated theoretical outcomes. Gels synthesized with a 10 mol% TFEA feed displayed the highest surface fluorine deviation ($55.1 \pm 12.3\%$) while those with 35 mol% TFEA fell below their anticipated value ($-43.2 \pm 31.3\%$). Standard polymers with 5 mol% feeds of DFHA ($0.0 \pm 24.5\%$), TFEA ($0.0 \pm 24.1\%$), and HFIA ($0.0 \pm 41.7\%$) all held closely to their average projected fluorine content but with notably high error. To test whether the relatively polar, hydrophilic SiO_2 surface of glass caused internalization of TFEA at higher feed concentrations, the depth profile for gels synthesized with a 35 mol% feed was scanned and presented in Figure 1 (b). Compared to the low ($6.8 \pm 3.7\%$)

fluorine composition of their surface, the high TFEA feed gels demonstrated increased fluorine content throughout their depth (from $12.1 \pm 1.8\%$ to $13.2 \pm 1.6\%$). Variability along the depth profile remains within error between individual points, but the rise in fluorine content at the gel surface potentially indicates a shallow TFEA concentration gradient at high comonomer feed extremes.

3.2 Swelling Analysis

Building from the high sensitivity of PNIPAM gels toward TPFOS relative to other surfactants and hydrotropes at comparable concentrations explored previously,⁹ gels copolymerized with 5 mol% feed DFHA, TFEA, and HFIA were exposed to the same chemical survey to identify whether the addition of fluorinated comonomers to the network would exploit fluorine-fluorine attraction to enhance the network's responsiveness toward fluorinated analytes. Complementing prior observations of augmented swelling in solutions of 1 mM TPFOS, each fluorinated gel exhibited significantly higher swelling in the presence of TPFOS compared to 1 mM solutions of OA, SDS, Ph, and SOS, a 10 mM solution of MeOH, and a 1 mM solution of PFOA with 10 mM MeOH (see Supplementary Figure 6). Viewing swelling ratios in terms of their difference to a DI water control for each gel (shown in Figure 2 (a)), the systems demonstrate maximal swelling differences of $3,201 \pm 466\%$, $3,100 \pm 197\%$, $3,378 \pm 173\%$, and $2,426 \pm 284\%$ at $35\text{ }^\circ\text{C}$ for BG, D5.0, T5.0, and H5.0, respectively, with TPFOS. Maximal differences are, at best, two orders of magnitude lower for all other analytes tested (see Supplementary Figure 7 for magnification of Figure 2 (a)) with T5.0 exposed to SDS showing the highest difference ($80 \pm 15\%$) at $25\text{ }^\circ\text{C}$ and BG mixed with OA holding the lowest difference ($-37 \pm 8\%$) at $32.5\text{ }^\circ\text{C}$. The location of the maximal swelling difference for TPFOS occurs at the temperature step just prior to rapid deswelling, or the onset of swelling change acceleration (see Supplementary Figure 8). Flattening of the water swelling ratio curve for each gel at approximately $32.5\text{ }^\circ\text{C}$ is met by relative quiescence of their TPFOS curves, and the abrupt change in TPFOS trajectory thereafter marks the maximum difference for each system. From the four gels tested, T5.0 presents the highest maximum swelling difference of $3,378 \pm 173\%$ with an AUC (1.272 ± 0.072) across the temperature range examined bested by only D5.0 (1.491 ± 0.092). Prioritizing maximal sensitivity to the analyte of interest over potential improvement in linearity reflected by a larger AUC, TFEA was selected as the comonomer for further examination.

Testing the influence of TPFOS specifically, gels with TFEA feeds ranging from 2.5 mol% to 35 mol% were subject to 1 mM concentrations of the analyte and the resulting differences (derived from the swelling ratios in Supplementary Figure 9) are reported in Figure 2 (b). Slight alterations in the feed ratio of TFEA caused significant changes in both the maximum swelling difference of the gel, the position of maximal difference, and the TPFOS-induced AUC from $5\text{ }^\circ\text{C}$ to $50\text{ }^\circ\text{C}$, all of which are recorded in Table 2. Increasing the TFEA feed composition from 5 mol% to 10 mol% raised the maximum difference to $3,761 \pm 147\%$ with a $5\text{ }^\circ\text{C}$ drop in its temperature location, and the AUC accompanying the change (1.679 ± 0.094) was outcompeted only by furthering the feed to 12.5 mol% (1.772 ± 0.094). Fitting and normalizing trends for the maximum swelling ratio difference and the AUC across the

composition range used, optima between the two parameters were found at TFEA feed concentrations of 10.7 mol% and 16.2 mol% (see Supplementary Figure 10). The latter of the two compositions has lower extremes for both parameters, leading the former as the optimum TFEA composition for TPFOS sensitivity.

3.3 TPFOS Swelling Kinetics

Albeit useful for enhancing the polymer's responsiveness toward PFOS, raising the fluorine composition of gels could introduce unwanted diffusion limitations by increasing the innate hydrophobicity of the gels or restricting binding to surface adsorption rather than thorough absorption. To monitor potential restriction of analyte perfusion through the network, swelling kinetics of gels synthesized with 5 mol% (T5.0) to 15 mol% (T15.0) TFEA feeds were collected up to a sequential deviation of less than 1%. Equilibration times in 1 mM TPFOS solutions, marked in Figure 3 (a), display elongation from 48 h for T5.0 up to 244 h for T15.0. Fluorine-fluorine attraction and complementary hydrophobicity brought on by heightened TFEA content initially compress the network, impeding uptake of bulky PFOS molecules. Fluorosurfactant binding to the periphery of the gel in the manner detailed by Kokufuta et al.¹⁵ accompanied by multilayered repulsion in the same region hypothesized in our previous study⁹ lends to progressive network expansion that lengthens the equilibration time as the fluorine content of the gel increases. The curvature of the T15.0 gels expresses this phenomenon the most clearly: initially, water penetrates the network with little resistance. As PFOS binds to the rim of the gel and complexes, swelling facilitates further fluorosurfactant penetration towards the interior. The inflection between 72 h and 96 h likely indicates complete network saturation bolstered by subsequent multilayering. Increasing the TFEA feed concentration beyond 15 mol% serves to extend the time to 1,320 h for a 20 mol% gel (see Supplementary Figure 2), following a logarithmic trend ($r^2 = 0.993$) across the feed compositions tested.

If the diffusivity reduction was caused by initial network compression from fluorinated comonomers, analytes with lower molecular volume might breach the matrix more easily and accelerate swelling. Investigating this hypothesis, kinetics for PFBS, the four-carbon analog to PFOS currently used as an industry alternative, under the same concentration as TPFOS were monitored as shown in Figure 3 (b). Interestingly, the equilibrium swelling ratio for each gel after 48 h (20.2 ± 0.8 for T5.0, 9.6 ± 0.2 for T10.0, 5.8 ± 0.2 for T12.5, and 3.8 ± 0.2 for T15.0) is negligibly different from their swelling in water alone (21.7 ± 0.5 for T5.0, 9.9 ± 0.2 for T10.0, 5.7 ± 0.2 for T12.5, and 3.6 ± 0.1 for T15.0), suggesting that PFBS does not have an appreciable effect on the swelling or LCST of the gels. The relatively short tail length for PFBS raises its critical micelle concentration (CMC) significantly to 0.148 M¹⁶ relative to 1.1-7.5 mM for TPFOS^{17, 18} which, by raising its suitability for an aqueous environment, reflects lowered association to PNIPAM chains. Following the general rule for fluorosurfactants holding aggregation properties similar to hydrocarbon surfactants with 1.5 times longer carbon tails,¹⁷ the four-carbon PFBS would be expected to mirror C₆ alkyl surfactants that have no discernable effect on the transition temperature of PNIPAM at concentrations two orders of magnitude larger than those used here.¹⁹ Shortening the tail length enhances the contribution of the hydrophilic head

group to the surfactant, placing PFBS as a relatively hydrophilic molecule that presents lower partitioning to the gel than PFOS. These results agree with the attenuation of LCST perturbation at lowered tail lengths reported for non-fluorinated anionic surfactants,^{19, 20} but they do little to reconcile the mechanism behind elongated swelling kinetics for these gels.

3.4 TPFOS Titration Assessment

Assessing the influence of TFEA composition over the polymer dose-response behavior to TPFOS, T12.5 gels in Figure 4 demonstrate only slight normalized swelling loss between 1.0 mM TPFOS (1.00 ± 0.02) and 0.5 mM (0.67 ± 0.06) at 20 °C while stagnating below 0.5 mM. The trend is maintained at 35 °C (1.00 ± 0.06 to 0.69 ± 0.06) and eliminated by 45 °C (0.98 ± 0.06 to 0.91 ± 0.07), probably due to the short initial equilibration time (16 h) employed. Response attrition between temperatures below (20 °C) and above (45 °C) the polymer's undisturbed LCST could indicate binding inhibition or a transition to adsorption rather than perfused absorption.²¹ T2.5 and T5.0 gels, by contrast, have a linear response between 1.0 mM (1.00 ± 0.07 for T2.5 and T5.0) and 0.25 mM (0.51 ± 0.04 for T2.5, 0.46 ± 0.05 for T5.0) at 20 °C with attenuation below 0.25 mM. BG at the same temperature instead show a sharp decline in normalized swelling from 1.0 mM (1.00 ± 0.09) to 0.5 mM (0.32 ± 0.00) which levels thereafter. At elevated temperatures (i.e., 35 °C and 45 °C), all gels fed with ≤ 5 mol% TFEA display rapid decay in their response below 0.5 mM, likely due to their collapse at these temperatures which, again, alters uptake from thorough analyte penetration to limited adsorption. Given longer equilibration times, progressive expansion from complexation at the edges of the gel might eventually breach the diffusion barrier set at higher temperatures and allow for absorption into the network's confines, but the conditional variations necessary to explore uptake kinetics as a function of TFEA feed ratio and TPFOS concentration were not investigated here. Overall, relatively small additions of TFEA appear to enhance fluorinated analyte absorption while mitigating diminishing returns from innate polymer collapse and diffusion limitations at higher feed ratios (i.e., >5 mol%).

4. Discussion

4.1 Fluorosurfactant-induced polymer swelling is a function of multiple competing weak molecular associations.

Despite showing tunable swelling responses via inclusion of fluorinated comonomers, the mechanisms involved in promoting the interaction of PFAAs to PNIPAM hydrogels remain unclear. Surveying the literature reveals that adsorption strategies for removing PFAS from aqueous samples have previously seen improved retrieval of longer chained fluorinated species (approaching and above C₈) using fluorinated polymers as adsorbents,²²⁻²⁵ likely due to fluorinated compounds simultaneous hydrophobicity and oleophobicity. Repulsion from water together with weak intermolecular F-F interactions drives association between fluorinated chains stabilizes their attraction despite the electron withdrawing effect of fluorocarbons heightening their electron density.^{1, 26} When mixed with hydrocarbon constituents, additional hydrogen bonding and interfacial mechanisms owing to

the fluorine groups oleophobicity also become apparent.^{17, 26} The same phenomena are likely at play here, but their individual contributions are not easily discerned from the complex fluorocarbon-hydrocarbon copolymers employed in this study. Association discrepancies are likely the result of several disjointed phenomena such as the structure of the fluorine moieties (i.e., pendent CF_3 versus chained CF_2), individual monomer interactions effecting either the void volume or diffusion resistance within the polymer matrix, the overall maximal swelling capacity and interchain separation of the gel, and the polymer's thermodynamics following lowered NIPAM content in exchange for hydro- and oleophobic comonomers working in unison to attract fluorinated species to the gel. The influence of each potential contributing factor and their relative weight toward the overall observed swelling behavior is convoluted; geometric and chemical properties in the form of molecular weight, composite and individual Van der Waals volume, surface area, solvent-accessible surface area, and component fluorine content for each comonomer did not show strong association (i.e., $r^2 > 0.900$) with the TPFOS-induced maximal swelling difference, swelling ratio, LCST, or LCST shift (data not shown). Suppositions regarding principle contributing factors are surmisable, such as fluorinated moieties stimulating binding or initially compressing the network to accentuate the resultant expansion by TPFOS, but the discrete contributions of each matrix component is complicated by the system's tandem fluorine and thermodynamic responses. Further investigation is necessary to elucidate the affinity of each polymer for fluorosurfactants across the scope of operational temperatures to verify whether the enhanced swelling response is attributable to binding stimulated by fluorinated comonomers or the innate swelling differential between fluorinated and non-fluorinated gels.

4.2 The structure of fluorinated pendant chains heavily influence the swelling behavior of their corresponding gels.

Although TFEA was chosen as the primary comonomer for study, the set feed composition (5 mol%) used for initial swelling analyses might have masked optimal feed ratios for DFHA and HFIA. T5.0, in this case, was the only gel that surpassed the maximal swelling difference of BG, but the difference for TFEA gels was further improved by raising the comonomer feed ratio to 10 mol%. Were the trend similar for DFHA and HFIA gels, slight alterations in their feed ratio could potentially improve their sensitivity. Should the limits for both comonomers hide outside of their tested composition, the high AUC for D5.0 in particular could indicate broadening of the response range that could further improve linearity at lower TPFOS concentrations. If the attractiveness of fluorinated comonomers to fluorinated contaminants is a consequence of the gel's atomic composition, DFHA ratios comparable to the TFEA gels tested would show reasonably higher residues of absorption in the metrics examined. This phenomena would be offset by heightened hydrophobicity and premature gel collapse at the temperature issued, leaving the optimal compositions for alternative comonomers, as for TFEA, a question of balance between maximizing attractiveness in the form of favorable F-F association while minimizing the copolymer's intrinsic repulsion for aqueous environments.

Briefly assuming that comonomers are equally incorporated into their networks, the swelling ratio curves for H5.0 and T10.0 are remarkably similar when exposed to 1.0 mM TPFOS with only slight deviations between 40 °C and 42.5 °C (see Supplementary Figure 6 and Supplementary Figure 9). Comparison of D5.0 and T20.0 curves does, however, reveal considerable difference. Though both curves have similar initial swelling ratios at 5 °C, T20.0 linearly deswells across the temperature sweep, reaching a swelling ratio of 3.47 ± 1.31 by 35 °C while D5.0 demonstrates a rapid decay initiated at 37.5 °C resulting in a deswollen ratio of 4.26 ± 1.44 at 45 °C. If the assumption of equal comonomer incorporation remains serviceable, the TPFOS-induced swelling behavior of the gels would consequently be independent of the gels' total fluorine content. Rather, the structure of the comonomers appears to play a key role in defining their swelling response to TPFOS. Fluctuations in surface fluorine content from XPS in Figure 1 show TFEA-copolymerized gels holding higher total fluorine content than their theoretical loading would suggest and higher relative fluorine content than their compared non-TFEA gels. The similarity of the H5.0 and T10.0 curves despite potential deviations in their fluorine content reinforce the importance of the comonomer morphology in determining the influence of TPFOS on the gels' swelling.

Interestingly, the LCST in Table 2 for each gel fed with 5 mol% comonomer remains near that of BG (40.2 ± 0.8 °C). For T5.0 (39.1 ± 0.2 °C) and H5.0 (37.0 ± 0.3 °C), their values remain outside a single standard deviation, but still above their LCST in water (22.2 ± 0.2 °C for T5.0, 17.0 ± 0.7 °C for H5.0) by more than that of BG (15.3 ± 0.7 °C). The changes in LCST from 1 mM TPFOS relative to BG are less drastic than swelling differences for D5.0 and T5.0, whereby the TPFOS-induced LCST shift for D5.0 ($-0.4 \pm 1.9\%$) pales in comparison to its maximum swelling ($-28.8 \pm 9.3\%$) against BG. T5.0 likewise displays a much lower LCST change ($-2.6 \pm 1.7\%$) compared to its swelling ratio ($-16.8 \pm 10.6\%$), but H5.0 shows similar deviation between its LCST ($-8.0 \pm 1.7\%$) and swelling ($-7.0 \pm 14.0\%$). The non-branched systems (i.e., D5.0 and T5.0) appear to have decoupled physical and thermodynamic cues in response to TPFOS, indicating that TFEA and DFHA must exclude a greater amount of water than HFIA without disrupting surfactant binding pathways. The linear structure of DFHA, which is expectedly rigid owing to the shell of fluorine surrounding the carbon chain, mimics the tail of PFOS sufficiently to facilitate compaction amongst adjacent fluorosurfactant molecules during saturation, potentially compressing the network to a greater degree than structurally dissimilar species like TFEA and HFIA. TFEA, with its single carbon atom populated by fluorines, marginally disrupts packing amongst fluorosurfactant tails to permit greater solvent penetration into the network. The ellipsoidal character of HFIA's branched fluorine shell spreads adjacent fluorosurfactants more than TFEA, furthering solvent penetration while encumbering TPFOS alignment. Assuming the surfactant association mechanisms to the matrix (e.g., electrostatics, interfacial separation) are uninterrupted by fluorinated comonomers, the packing of fluorosurfactants absorbed to the network determines the resulting volume available for solvent and, consequently, the resulting swelling ratio for the polymer-surfactant system. This proposal follows in-line with considerations for tightly packed perfluorosulfonates favoring solvent-penetrated cylindrical micelles at high concentrations.^{1, 17}

^{27, 28} In this case, the driving forces behind fluorosurfactant reconfiguration and expulsion at higher temperatures allowing for collapse of the hydrogel would not differ significantly regardless of the comonomer used. The data for low comonomer feed ratios (i.e., ≤ 5 mol%) agree with this notion while larger fluorinated comonomer feeds become complicated by suppression of the copolymer's thermoresponsive portion, abundant fluorinated comonomer interplay, and innate polymer hydrophobicity that impedes overall swelling.

4.3 Detection of PFAAs using fluorine-containing thermoresponsive copolymers hinges upon a delicate balance between favorable interactions and suppression of the polymers' temperature responsiveness.

Notably, several barriers remain for the use of fluorinated PNIPAM hydrogels to sense fluorinated analytes, namely: implementing fluorinated comonomers in the network, as discussed earlier, reduces the maximum swelling capacity of the polymer, significantly prolongs equilibration times due to apparent diffusion limitations, and substitutes NIPAM binding domains for weak fluorine-fluorine attraction. The first two limitations have been detailed extensively thus far; the latter presents a tailorable tool for regulating the physiochemical response of the system. Although NIPAM moieties control the thermodynamic behavior of the gels, inclusion of fluorinated comonomers reduces the LCST for gels precipitously as the feed ratio of comonomer increases, possibly from nearby fluorine constituents disrupting the hydrophobic hydration or clathrate cage around the isopropyl groups of NIPAM. Preconditioned disorder in this domain would fuel entropy-driven demixing²⁹ and reduce the volume phase transition temperature of the system as this study's data illustrate. On the topic of analyte binding, the weak associations between fluorinated species,²⁶ likely from attractive van der Waals forces,¹ posts the advantage of reversibility should a hydrogel sensor be reusable but also the disadvantage of inefficacy for trace analysis. The relative strength of fluorine-fluorine association compared to the electrostatic association of fluorosurfactants with weakly polyelectrolytic PNIPAM alone is still unresolved.

From the swelling response of the gels tested, raising the fluorine content of the matrix did not appear to drastically alter the aggregation behavior of the fluorosurfactant to the gels. Employing swelling as a measure for the molecular association of fluorosurfactants to the polymer is, however, a coarse estimate of the phenomenon. In our previous study,⁹ association was found to occur at an order of magnitude lower concentration when monitored fluorimetrically. The initiation of swelling perturbations at 0.25 mM rather than 0.5 mM for T2.5 and T5.0 gels might, therefore, indicate slight lowering of the interpolated critical aggregation concentration. Additionally, implementing fluorinated comonomers did show changes in the response of gels at the highest TPFS concentration used, whereby the maximum swelling difference and AUC were raised, granting the method usefulness for designing the breadth of the polymer's response to fluorosurfactants. Further improvements in the form of ionic comonomers could facilitate additional binding to the network via electrostatics that, together with fluorinated comonomers, may

enhance the system's receptivity to the analyte of interest in future applications.

Conclusions

Incorporating fluorinated comonomers into the backbone of PNIPAM hydrogels served to provide a method for tailoring the responsiveness of the gels' swelling response toward fluorosurfactants through a delicate balance of comonomer selection and feed ratio optimization. As a sensing tool, a TFEA comonomer feed of 10.7 mol% was estimated to maximize the water-analyte swelling difference and AUC exhibited by the polymer in the presence of TPFS from 5 °C to 50 °C. Raising feed ratios of TFEA was shown to broaden the swelling response range for the gels at the expense of reduced overall swelling ratios and exacerbated equilibrium times, opening a window for tuning the network's behavior with small (≤ 2.5 mol%) changes in comonomer feed ratio. Further, high feed concentrations of TFEA led to internalization of fluorinated monomers within the gel matrix, forwarding the symptoms of elongated equilibration as a consequence of a radially defined diffusion barrier synchronized with the penetration inhibition mechanisms described by Kokufuta et al.¹⁵ Improvement to the system in the form of ionic comonomers used to capitalize on the electroactive head groups of fluorosurfactants in conjunction with fluorinated comonomers to exploit their fluorophilicity presents an avenue for continued honing of the polymer's physiochemical properties as a means to alert the presence of concerning fluorinated analytes.

Conflicts of interest

The authors declare no conflicts of interest.

Acknowledgements

Access to characterization instruments and staff assistance was provided by the Electron Microscopy Center at the University of Kentucky, supported in part by the National Science Foundation/EPSCoR Award No. 1355438 and by the Commonwealth of Kentucky.

Research reported was supported by NIEHS/NIH grant P42ES007380. The content is solely the responsibility of the authors and does not necessarily represent the official views of the NIH.

References

1. F. Giulieri and M.-P. Krafft, *Colloids and Surfaces A: Physicochemical and Engineering Aspects*, 1994, **84**, 121-127.
2. *Journal*, 2018.
3. J. P. Giesy and K. Kannan, *Environmental Science & Technology*, 2001, **35**, 1339-1342.
4. R. C. Buck, J. Franklin, U. Berger, J. M. Conder, I. T. Cousins, P. de Voogt, A. A. Jensen, K. Kannan, S. A.

- Mabury and S. P. van Leeuwen, *Integrated Environmental Assessment and Management*, 2011, **7**, 513-541.
5. J.-M. Jian, Y. Guo, L. Zeng, L. Liang-Ying, X. Lu, F. Wang and E. Y. Zeng, *Environment International*, 2017, **108**, 51-62.
6. Z. Wang, I. T. Cousins, M. Scherlinger, R. C. Buck and K. Hungerbühler, *Environment International*, 2014, **70**, 62-75.
7. *Journal*, 2017.
8. *Journal*, 2018.
9. D. T. Savage, N. J. Briot, J. Z. Hilt and T. D. Dziubla, *Journal of Polymer Science*, 2021, **59**, 289-299.
10. M. H. Futscher, M. Philipp, P. Müller-Buschbaum and A. Schulte, *Scientific Reports*, 2017, **7**, 17012.
11. R. A. Nyquist, S. Fiedler and R. Streck, *Vibrational Spectroscopy*, 1994, **6**, 285-291.
12. D. V. Le, M. M. Kendrick and E. A. O'Rear, *Langmuir*, 2004, **20**, 7802-7810.
13. A. Kadimi, H. Kaddami, Z. Ounaies, Y. Habibi, R. Dieden, B. Ameduri and M. Raihane, *Polymer Chemistry*, 2019, **10**, 5507-5521.
14. K. P. Huang, P. Lin and H. C. Shih, *Journal of Applied Physics*, 2004, **96**, 354-360.
15. E. Kokufuta, H. Suzuki and D. Sakamoto, *Langmuir*, 1997, **13**, 2627-2632.
16. ECOTOXICOLOGY AND ENVIRONMENTAL FATE TESTING OF SHORT CHAIN PERFLUOROALKYL COMPOUNDS RELATED TO 3M CHEMISTRIES, Report Exhibit 2231, Hennepin County District Court, 2008.
17. E. Kissa, *Fluorinated Surfactants and Repellents, Second Edition*, Taylor & Francis, 2001.
18. G. Gente, C. La Mesa, R. Muzzalupo and G. A. Ranieri, *Langmuir*, 2000, **16**, 7914-7919.
19. M. Sakai, N. Satoh, K. Tsujii, Y.-Q. Zhang and T. Tanaka, *Langmuir*, 1995, **11**, 2493-2495.
20. H. G. Schild and D. A. Tirrell, *Langmuir*, 1991, **7**, 665-671.
21. Y. Murase, T. Onda, K. Tsujii and T. Tanaka, *Macromolecules*, 1999, **32**, 8589-8594.
22. M. Takayose, K. Nishimoto and J. Matsui, *Analyst*, 2012, **137**, 2762-2765.
23. Z. Yan, Y. Cai, G. Zhu, J. Yuan, L. Tu, C. Chen and S. Yao, *Journal of Chromatography A*, 2013, **1321**, 21-29.
24. Z. Yan, G. Zhu, Y. Cai, J. Yuan and S. Yao, *Analytical Methods*, 2015, **7**, 9054-9063.
25. L. Xiao, Y. Ling, A. Alsbaiee, C. Li, D. E. Helbling and W. R. Dichtel, *Journal of the American Chemical Society*, 2017, **139**, 7689-7692.
26. R. J. Baker, P. E. Colavita, D. M. Murphy, J. A. Platts and J. D. Wallis, *The Journal of Physical Chemistry A*, 2012, **116**, 1435-1444.
27. A. Knoblich, M. Matsumoto, K. Murata and Y. Fujiyoshi, *Langmuir*, 1995, **11**, 2361-2366.
28. X. Wang, J. Chen, D. Wang, S. Dong, J. Hao and H. Hoffmann, *Advances in Colloid and Interface Science*, 2017, **246**, 153-164.
29. I. Bischofberger, D. C. E. Calzolari and V. Trappe, *Soft Matter*, 2014, **10**, 8288-8295.

ARTICLE

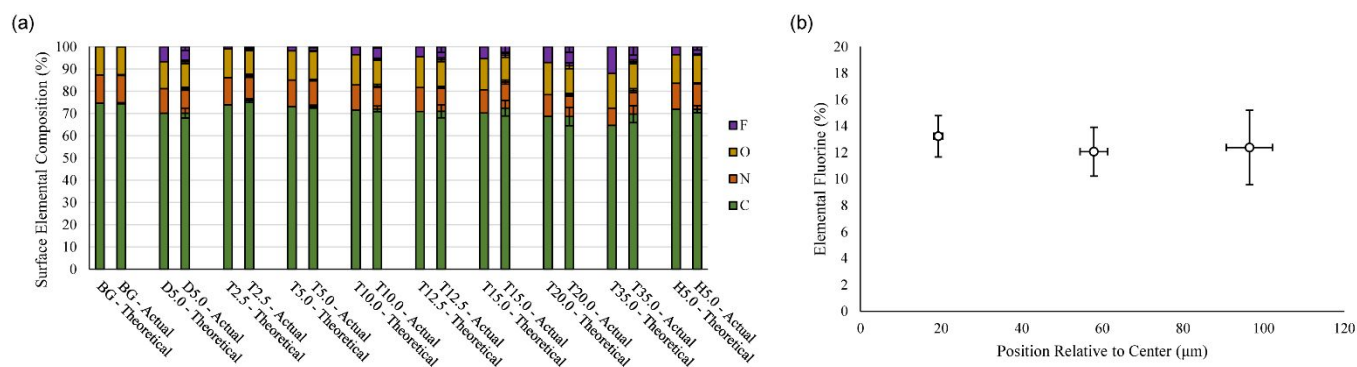


Figure 1: Surface elemental analysis for all gels studied (a) and atomic fluorine depth profile for gels synthesized with a 35 mol% TFEA feed (b). Disks examined in (b) had approximate thicknesses of 220 μm. Survey results in (a) show the compositional average and standard deviation for two points of one gel from three batches. Line scans in (b) likewise result from two points scanned across the thickness of a single gel taken from three separate batches.

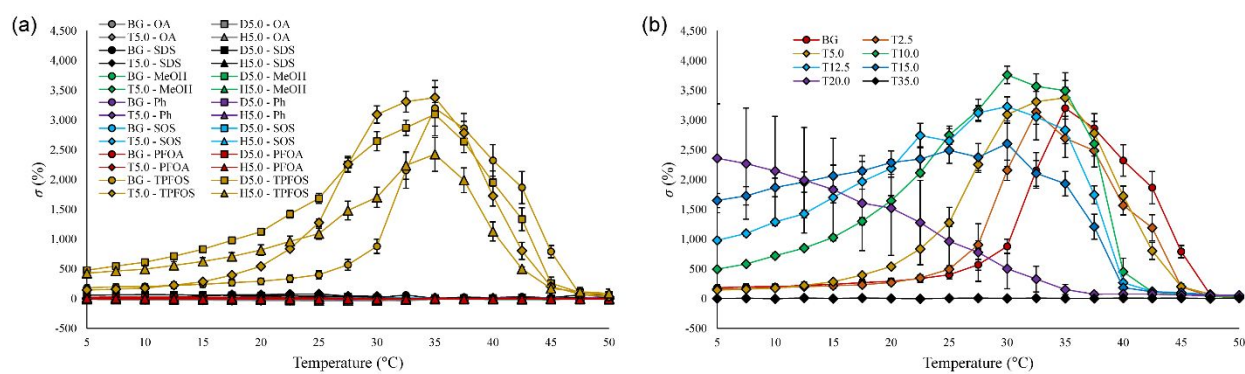


Figure 2: Water-analyte swelling differences for (a) gels without a comonomer (BG) and those with 5 mol% comonomer feeds exposed to 1 mM OA (gray), 1 mM SDS (black), 10 mM MeOH (green), 1 mM Ph (purple), 1 mM SOS (light blue), 1 mM PFOA with 10 mM MeOH (red), and 1 mM TPPOS (gold) and (b) gels synthesized with varying TFEA feeds soaked in solutions of 1 mM TPPOS. Error bars represent a single standard deviation for $n = 3$ gels.

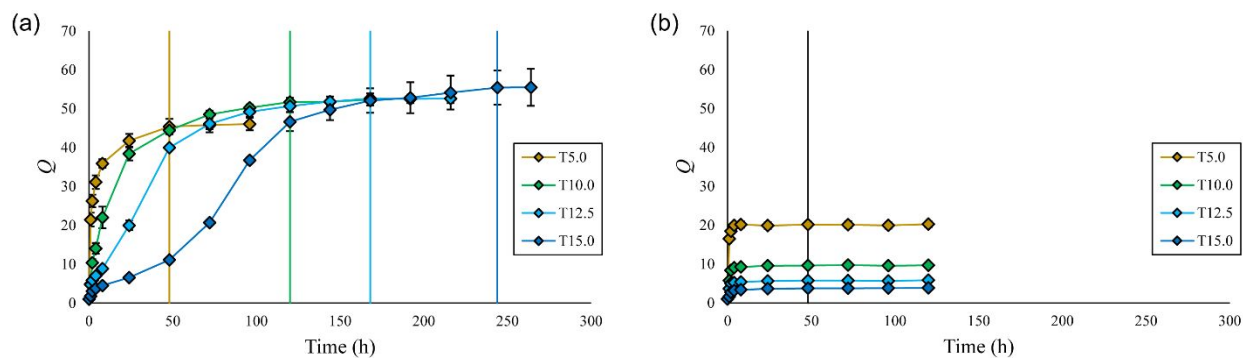


Figure 3: Swelling ratios for TFEA copolymers soaked in (a) 1 mM TPFS and (b) 1 mM PFBS solutions at 5 °C. Lines are meant to guide the eye to the equilibrium time (<1% deviation) for each system. Error bars represent the standard deviation for $n = 3$ gels.

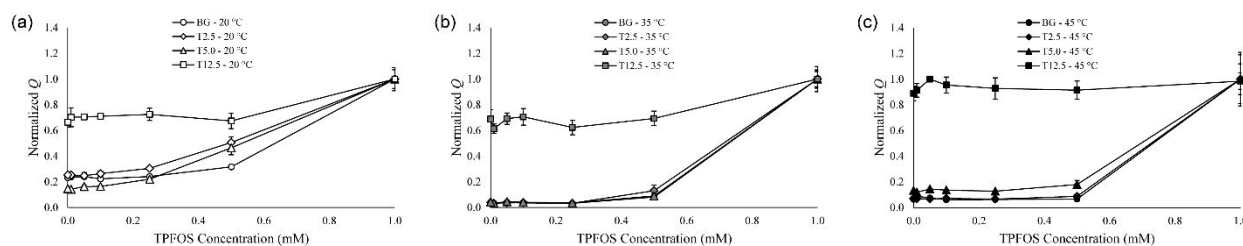


Figure 4: Normalized swelling ratios for gels fed with zero (circles), 2.5 mol% (diamonds), 5.0 mol% (triangles), and 12.5 mol% (squares) TFEA exposed to varying concentrations of TPFS for 16 h at (a) 20 °C, (b) 35 °C, and (c) 45 °C. Error bars represent a single standard deviation from $n = 3$ gels.

ARTICLE

Journal Name

Table 1: Gel synthesis conditions and corresponding acronyms for each system. Title acronyms correspond to the component order (Comp.), total monomer concentration (TMC), and initiator concentration (I). Both non-fluorinated (BG) gels synthesized from *N*-isopropylacrylamide (NIPAM) and *N,N'*-methylenebis(acrylamide) (MBA) alone and those formed with varying feed ratios of 2,2,2-trifluoroethyl acrylate (TFEA), 1*H*,1*H*,7*H*-dodecafluoroheptyl acrylate (DFHA), and 1,1,1,3,3,3-hexafluoroisopropyl acrylate (HFIA) are presented (i.e., D5.0, T2.5 through T35.0, and H5.0).

Acronym	Comp. 1	Comp. 2	Comp. 3	mol% 1	mol% 2	mol% 3	TMC (M)	I (mM)
BG	NIPAM	MBA	-	97.54	2.46	-	1.29	12.38
D5.0	NIPAM	MBA	DFHA	92.54	2.46	5.00	1.30	12.47
T2.5	NIPAM	MBA	TFEA	95.04	2.46	2.50	1.30	12.47
T5.0	NIPAM	MBA	TFEA	92.54	2.46	5.00	1.30	12.47
T10.0	NIPAM	MBA	TFEA	87.54	2.46	10.00	1.30	12.47
T12.5	NIPAM	MBA	TFEA	85.04	2.46	12.50	1.30	12.47
T15.0	NIPAM	MBA	TFEA	82.54	2.46	15.00	1.30	12.47
T20.0	NIPAM	MBA	TFEA	77.54	2.46	20.00	1.30	12.47
T35.0	NIPAM	MBA	TFEA	62.54	2.46	35.00	1.30	12.47
H5.0	NIPAM	MBA	HFIA	92.54	2.46	5.00	1.30	12.47

Table 2: List of the temperature at half maximum swelling ratio (LCST) in water and in 1 mM TPFOS, their corresponding difference, and the AUC, maximum, and temperature at which the maximum occurs for the water-analyte swelling difference of each gel used in this study. Error represents a single standard deviation for $n = 3$ samples where applicable.

	H ₂ O LCST (°C)	TPFOS LCST (°C)	LCST Rise (°C)	Normalized AUC	Max σ (%)	Max σ Temp. (°C)
BG	24.9 ± 0.2	40.2 ± 0.8	15.3 ± 0.7	1.000 ± 0.123	3,201 ± 466	35.0
D5.0	17.6 ± 0.2	40.0 ± 0.4	22.4 ± 0.4	1.491 ± 0.092	3,100 ± 197	35.0
T2.5	22.6 ± 0.1	39.7 ± 0.5	17.2 ± 0.4	0.977 ± 0.110	3,137 ± 466	32.5
T5.0	16.9 ± 0.1	39.1 ± 0.2	22.2 ± 0.2	1.272 ± 0.072	3,378 ± 173	35.0
T10.0	14.4 ± 0.1	37.6 ± 0.1	23.2 ± 0.1	1.679 ± 0.094	3,761 ± 147	30.0
T12.5	15.6 ± 0.4	35.9 ± 0.2	20.3 ± 0.4	1.772 ± 0.094	3,227 ± 166	30.0
T15.0	21.7 ± 0.9	32.4 ± 0.3	10.7 ± 0.8	1.674 ± 0.159	2,605 ± 381	30.0
T20.0	N/A	21.5 ± 3.2	N/A	0.997 ± 0.478	2,360 ± 916	5.0
T35.0	N/A	N/A	N/A	0.007 ± 0.008	12 ± 12	12.5
H5.0	20.0 ± 0.7	37.0 ± 0.3	17.0 ± 0.7	1.044 ± 0.095	2,426 ± 284	35.0